Article

Antimalarial Activity of Highly Coordinative Fused Heterocycles Targeting β-Hematin Crystallization

María E. Acosta, Lourdes Gotopo, Neira Gamboa, Juan R. Rodrigues, Genesis C. Henriques, Gustavo Cabrera, and Angel H. Romero*

Read Online

ACCESS | Metrics & More | Article Recommendations | Supporting Information

ABSTRACT: The β-hematin formation is a unique process adopted by *Plasmodium* sp. to detoxify free heme and represents a validated target to design new effective antimalarials. Most of the β-hematin inhibitors are mainly based on 4-aminoquinolines, but the parasite has developed diverse defense mechanisms against this type of chemical system. Thus, the identification of other molecular chemical entities targeting the β-hematin formation pathway is highly needed to evade resistance mechanisms associated with 4-aminoquinolines. Herein, we showed that the highly coordinative character can be a useful tool for the rational design of antimalarial agents targeting β-hematin crystallization. From a small library consisting of five compound families with recognized antitrypanosomatid activity and coordinative abilities, a group of tetradentate 1,4-disubstituted phthalazin-aryl/heteroarylhydrazinyl derivatives were identified as potential antimalarials. They showed a remarkable curative response against *Plasmodium berghei*-infected mice with a significant reduction of the parasitemia, which was well correlated with their good inhibitory activities on β-hematin crystallization (IC_{50} = 5−7 μM). Their *in vitro* inhibitory and *in vivo* responses were comparable to those found for a chloroquine reference. The active compounds showed moderate *in vitro* toxicity against peritoneal macrophages, a low hemolysis response, and a good *in silico* ADME profile, identifying compound **2f** as a promising antimalarial agent for further experiments. Other less coordinative fused heterocycles exhibited moderate inhibitory responses toward β-hematin crystallization and modest efficacy against the *in vivo* model. The complexation ability of the ligands with iron(III) was experimentally and theoretically determined, finding, in general, a good correlation between the complexation ability of the ligand and the inhibitory activity toward β-hematin crystallization. These findings open new perspectives toward the rational design of antimalarial β-hematin inhibitors based on the coordinative character as an alternative to the conventional β-hematin inhibitors.

Highly coordinative system

2f
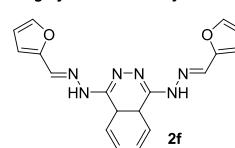
High complexation ability with iron (III)
High Inhibition of β-hematin: IC_{50} = 5.50 μM
Low cytotoxicity (macrophage): CC_{50} = 111.45 μM
Low hemolysis (RBCs): 22.13 % at 100 mM
Convenient *Log P* = 2.69
Convenient ADME properties

High curative response (29 days)
High parasitemia reduction (0.32 %)

INTRODUCTION

Malaria is a life-threatening disease caused by parasites of the genus *Plasmodium* spp., which is transmitted to humans through the bites of infected female *Anopheles* mosquitoes. It is one of the largest tropical diseases worldwide, registering an estimate of 241 million cases of malaria and 627,000 deaths in 2020 according to World Health Organization (WHO). From that statistics, it is important to mention that most of malaria deaths are associated with children aged less than 5 years with 67% of all malaria deaths worldwide.[1]

Talking about the *Plasmodium* parasite, it infects the red blood cells (RBCs) in mammals and it is able to consume more than 60−80% of hemoglobin during its erythrocytic stage.[2,3] From the hemoglobin digestion, the parasite releases a globin protein and heme group [ferriprotoporphyrin IX (FPIX)]. The first is useful as a nutrient source for the parasite, whereas the second species is highly toxic for the parasite with the capacity to induce membrane rupture. To overcome it, the parasite has developed a detoxification

mechanism within its digestive vacuole where the heme group is converted into a nontoxic crystalline solid called hemozoin (β-hematin), which is insoluble and can be eliminated via excretion.[4−6] The β-hematin solid is formed by noncovalent interaction between several molecules of the heme group, which are connected through hydrogen bonding interaction between the vicinal carboxylic moiety of two heme groups and the dimer unit (Figure 1A). The latter makes the inhibition of the β-hematin crystallization an important chemical target to design new antimalarial agents.[6−8] Diverse investigations have put in evidence that 4-aminoquinoline is a convenient scaffold to design new antimalarial agents.
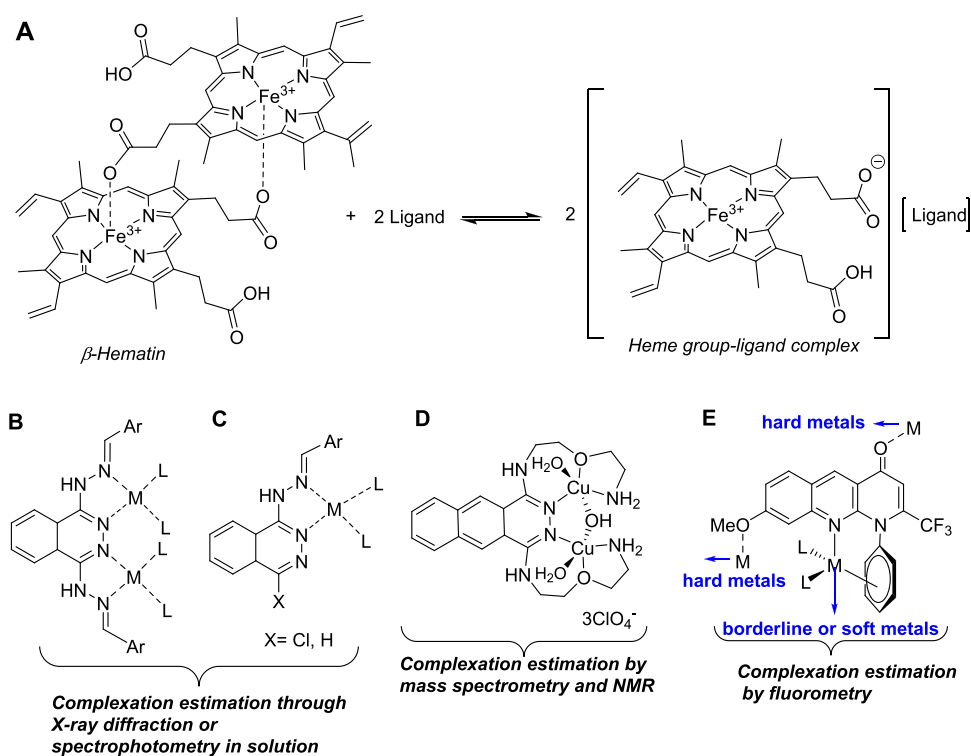
Figure 1. Scheme for the dissociation of β-hematin by ligand interaction (A), complexation modes of phthalazine-hydrazones (B, C), benzo[*g*]phthalazine functionalized with a nitrogen-rich chain (D), and *N*[1]-aryl-2-trifluoromethylbenzo[*b*]naphthyridin-4(1*H*)-ones (E).

Specifically, chloroquine (CQ) has been identified as one of the most important antimalarials targeting β-hematin crystallization. Other clinically 4-aminoquinolines including amodiaquine, quinine, and mefloquine have been recognized to inhibit the formation of β-hematin.[6−8] Also, an extended group of 4-aminoquinolines have been developed as an inhibitor of the formation of β-hematin.[7−12] Although the mechanism of inhibition of the formation of β-hematin is not well understood, diverse experimental and theoretical evidence has suggested that 4-aminoquinolines are able to block the formation of a β-hematin dimer through a π−π stacking interaction between the porphyrin ring of β-hematin and the quinoline ring. It facilitates an effective accumulation of the heme/drug complex within the erythrocyte, causing parasite death by oxidative stress.[7,8]
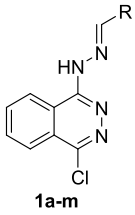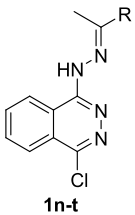
However, the parasite has developed a defense mechanism against quinoline-based drugs, which consists of preventing the accumulation of this type of agent within the vacuole of the parasite through the development of a mutation known as PfCRT, a membrane protein placed into the digestive food vacuole.[6,13−15] It has favored the resistance and survival ability of the parasite by treatment with quinolone-based agents. To counteract it, some structurally complex 4-aminoquinolines bearing a CQ-reverser such as verapamil, promethazine, chlorpheniramine, or primaquine have been developed and proved against resistant *Plasmodium* strains,[16] but that strategy remains insufficient. As a consequence, the discovered novel nonquinolinic systems targeting the inhibition of β-hematin crystallization with the ability to prevent the resistance mechanism of the parasite are highly needed as an alternative to 4-aminoquinolines.

To design a solid strategy, it is important to take into account the possible routes relative to the blocking of β-hematin crystallization. From experimental evidence, there are two interacting routes to block β-hematin crystallization: (i) π−π stacking between the aromatic ring of the inhibitor and the porphyrin ring of the heme group by using fused-aromatic systems and (ii) direct interaction of the iron(III) metal with the heme group complex. Justly, from Egan's report, 4-aminoquinolines act through a combined interacting route, finding proximity between the iron metal of the heme group and quinolinic nitrogen from theoretical simulation.[7] Then, the ability of the organic ligand to form a stable complex with iron(III) may be an interesting strategy to identify new nonquinoline antimalarials targeting β-hematin crystallization. The heme group contains an iron(III) metallic atom and its potential interaction with a coordinative agent may contribute to the degradation of the β-hematin dimer, releasing the desired toxic and soluble heme group within the parasite vacuole (Figure 1A).

From the literature, we found that diverse types of heterocyclic systems (*e.g.*, pyridine, xanthones, imidazoles, phenothiazinium salt, quinolin-4(1*H*)-ones, chromones, lumefantrine, halofantrine, and benzimidazoles) featuring a coordinative *N*-alkyl chain have been demonstrated to be good inhibitors of the β-hematin crystallization with relevant antimalarial activity.[17−20] Recently, a number of heterocycles bearing a highly coordinative chain-like hydrazone moiety have shown good inhibitory activity toward the β-hematin crystallization pathway.[21−26] With all information in mind, herein, we proved the ability of a series of highly coordinative heterocycles from a small molecule library to inhibit the formation of β-hematin as well as its potential as an antimalarial by using an *in vivo* model of *P. berghei*. The library is composed of 66 active compounds including a hit of 1-arylhydrazinyl-phthalazine, a hit of 1,4-diarylhydrazinyl-phthalazine, a hit of 3-aryl-6-(*N*′-methylpiperazine)[1,2,4]-triazolo[3,4-*a*]phthalazine, a hit of weak coordinative *N*[1]-aryl-

Table 1. Inhibitory Activity on Heme Crystallization (IHC) for the 1-Arylhydrazinyl-phthalazines (1a–1t) with Corresponding Log P Values

Entries	Compounds	-R	Code	IC$_{50}$ (μM), (%HIC)	Log P[a]
1		-C$_6$H$_5$ (Phenyl)	1a	15.93 ± 1.26	4.30
2		-p-C$_6$H$_4$F	1b	> 50.0	4.46
3		-p-C$_6$H$_4$Cl	1c	> 50.0	**4.86**
4		-p-C$_6$H$_4$Br	1d	11.34 ± 2.62	**5.13**
5		-p-C$_6$H$_4$NO$_2$	1e	13.99 ± 2.40	3.86
6	**1a-m**	-m-C$_6$H$_4$Cl	1f	28.79 ± 3.17	**4.86**
7		-m-C$_6$H$_4$Br	1g	> 50.0	**5.13**
8		-m-C$_6$H$_4$NO$_2$	1h	14.06 ± 2.21	3.86
9		-o-C$_6$H$_4$OH	1i	> 50.0	3.91
10		-2-OMe,4-NO$_2$-C$_6$H$_3$	1j	> 50.0	3.99
11		-C$_5$H$_3$O (Furyl)	1k	28.80 ± 2.56	2.92
12		-5-NO$_2$-C$_5$H$_2$O	1l	> 50.0	2.94
13		-5-NO$_2$-C$_5$H$_2$S	1m	> 50.0	3.43
14		-C$_6$H$_5$ (Phenyl)	1n	> 50.0	3.87
15		-p-C$_6$H$_4$OH	1o	> 50.0	3.48
16		-p-C$_6$H$_4$Br	1p	> 50.0	**4.70**
17	**1n-t**	-p-C$_6$H$_4$NO$_2$	1q	> 50.0	3.82
18		-m-C$_6$H$_4$NO$_2$	1r	> 50.0	3.82
19		-2,4-Cl$_2$-C$_6$H$_3$	1s	> 50.0	**4.98**
20		-2,5-Cl$_2$-C$_6$H$_3$	1t	> 50.0	**4.98**

[a]Red bold text indicates up-borderline Log P according to Lipinsky's rule.

2-trifluoromethylbenzonaphthyridin-4(1H)-ones, and a hit of noncoordinative 2-arylquinazolin-4(3H)-ones as a negative control. All these compounds were previously synthesized and evaluated against *in vitro* models of *Trypanosome cruzi* and *Leishmania* spp. parasites.[27−33] These parasites are responsible for Leishmaniasis and Chagas disease, respectively, and they, in conjunction with malaria, belong to the group of neglected tropical diseases.[34] Despite the genetic and host preference differences between the trypanosomatids and the *Plasmodium* parasites,[34] it is common to find antitrypanosomatid agents with good antimalarial activity.[35,36]
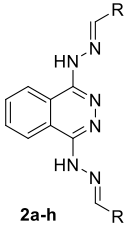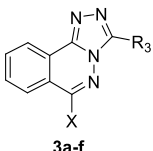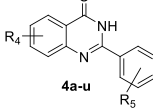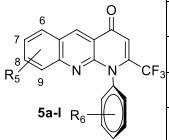
RESULTS AND DISCUSSION

Coordinative Character of the Tested Compounds. Our principle for the discovery of new inhibitors of β-hematin crystallization was based on the complexation ability of the molecular system with transition metals, in particular with the iron(III) ion. The latter is essential because the complexation ability of the ligand toward the iron(III) ion of the heme group may compromise the intermolecular interaction between multiple heme groups within the β-hematin crystal (*e.g.*, π−π stacking between porphyry rings), affecting its molecular integrity and releasing the toxic heme group (Figure 1A).[37] In our study, we selected a group of five families of compounds (1a−1t, 2a−2h, 3a−3f, 4a−4u, and 5a−5l): three of them as flexible systems possessing coordinative nitrogen chains (1a−1t, 2a−2h, and 3a−3f), a semiflexible ligand like *N*[1]-aryl-2-trifluoromethylbenzo[*b*]naphthyridin-4(1H)one, which may be able to form a half-sandwich complex (Figure 1E), and finally, a noncoordinative system of 2-arylquinazolin-4(3H)-

ones (Figure S1). The purpose of that selection is to analyze the relevance of the coordination character on the inhibition of β-hematin crystallization for an *in vitro* assay.

To have a preliminary knowledge relative to the coordination ability of the ligand with iron(III), we made an analysis from the HSAB (hard soft acid−base) theory. From the HSAB theory, the iron(III) metal is considered as a hard metal with a borderline character in some cases.[38] Then, analyzing the coordination character of our ligands, iron(III) should be able to form a stable complex with the ligands 1a−1t and 2a−2h because they contain a borderline basic moiety such as the hydrazinyl scaffold with a chelating environment that favors the stabilization of the metallic complex as bidentate and tetradentate ligands, respectively.[38] It is well documented that tetradentate ligands like 1,4-diarylhydrazi-nylphthalazines are able to form mononuclear and dinuclear complexes with hard transition metals like vanadium(IV), molybdenum(IV), and molybdenum(V) (Figure 1B).[39−42] Other complexes of Hg(II), Ni(II), Co(II), Pd(II), Cu(II), Ag(I), Zn(II), Cd(II), Mn(II), and Fe(III) have been reported for the monoarylhydrazinyl-phthalazines in a solid state or solution (Figure 1C).[43] Other phthalazine analogues featuring a nitrogen chain at the 1- or 4-position of the pyridazine core have been demonstrated to be able to form a complex with hard/borderline transition metals like manganese(II), cobalt-(II), cobalt(III), iron(II), nickel(II), copper(II), zinc(II), and mercury(II).[44−51] All evidence highlights the potential of the phthalazines 1a−1t and 2a−2h to form a complex with iron$^{2+/3+}$ species.

Table 2. Inhibitory Activity on Heme Crystallization (IHC) for the 1,4-Arylhydrazinyl-phthalazines 2a−2h, 1,2,4-Triazolophthalazines 3a−3f, 2-Arylquinazolin-4(3H)ones 4a−4u, N^1-Aryl-2-(trifluoromethyl)benzo[b][1,8] Naphthyridin-4(1H)-ones 5a−5l, and Chloroquine (CQ) with Corresponding Log P Values

Entries	Compounds	-R	Code	IC_{50} (μM), (%IHC)	Log P^a
21		-C_6H_5 (Phenyl)	2a	7.24 ± 0.03	4.01
22		-p-C_6H_4F	2b	7.10 ± 0.02	**4.58**
23		-p-$C_6H_4NO_2$	2c	> 50.0 (18.2)	2.56
24	2a-h	-m-$C_6H_4NO_2$	2d	5.80 ± 0.04	2.56
25		-o-C_6H_4OH	2e	5.30 ± 0.02	3.13
26		-C_5H_3O (Furyl)	2f	5.50 ± 0.01	2.69
27		-5-NO_2-C_5H_2S	2g	> 50.0 (11.3)	3.22
28		-5-NO_2-C_5H_2O	2h	8.51 ± 0.07	1.74
29		X,R_3=Cl, -C_6H_4F	3a	> 50.0 (15.4)	4.37
30		X,R_3=MeNCH$_2$CH$_2$N-, -C_6H_5	3b	17.66 ± 0.04	2.97
31	3a-f	X,R_3=MeNCH$_2$CH$_2$N-, -p-C_6H_4F	3c	15.60 ± 0.04	3.07
32		X,R_3=MeNCH$_2$CH$_2$N-, -p-$C_6H_4NO_2$	3d	> 50.0 (11.9)	3.53
33		X,R_3=MeNCH$_2$CH$_2$N-,-m-$C_6H_4NO_2$	3e	> 50.0 (13.5)	3.53
34		X,R_3=MeNCH$_2$CH$_2$N-, -C_5H_3O	3f	> 50.0 (37.6)	2.69
35-55	4a-u	See structures in Figure S1	4a-u	> 50.0	
56		R_5,R_6= 8-OMe, H	5a	9.70 ± 0.02	4.36
57		R_5,R_6=8-OMe, 4-Cl	5b	>50.0 (35.7)	**4.70**
58		R_5,R_6= 8-OMe, 3-OMe	5c	>50.0 (28.2)	4.01
59		R_5,R_6= 8-OMe, 4-Me	5d	>50.0 (9.2)	**4.63**
60		R_5,R_6=8-OMe, 4-OMe	5e	>50.0 (31.9)	4.01
61	5a-l	R_5,R_6= 8-Me, H	5f	>50.0 (26.8)	**4.75**
62		R_5,R_6= H, H	5g	>50.0 (21.2)	4.27
63		R_5,R_6= H, 4-Cl	5h	>50.0 (25.2)	**4.83**
64		R_5,R_6= 7-Me, H	5i	>50.0 (20.0)	**4.75**
65		R_5,R_6= 7-OMe, H	5j	>50.0 (35.2)	4.14
66		R_5,R_6= 7-OMe, 4-Cl	5k	11.80 ± 0.02	**4.70**
67		R_5,R_6= 7-OMe, 4-OMe	5l	>50.0 (39.8)	4.01
68	CQ			1.48 ± 0.01	3.05

^{a}Red bold text indicates up-borderline Log P according to Lipinsky's rule.

Regarding 3-aryl-6-(N'-methylpiperazine)-1,2,4-triazolophthalazines 3a−3f, we expected that they may act as a bidentate ligand with a hard character, which may complex with iron(III) through N'-methyl terminal nitrogen and N-heterocycle at the 5-position of the 1,2,4-triazolophthalazine core. Some examples of dinuclear copper(II) complexes in solution have been reported for phthalazine systems featuring dialkylamine chains (Figure 1D).[52] Recently, we reported that the 3-aryl-6-(N-methylpiperazine)-1,2,4-triazolophthalazine system acts as an inhibitor of the potassium channel for *in vitro* models of cancer cells, which suggests a tentative interaction of the potassium ion with the architecture of the mentioned heterocycle.[53]

Meanwhile, the N^1-(4-chlorophenyl)-2-trifluoromethyl-8-methoxybenzo[b]naphthyridin-4(1H)one is a relatively novel chemical system, and no reports exist about its complexation ability with transition metals. From theoretical calculations herein, we found that the N^1-aryl-2-trifluoromethylbenzo[b]-naphthyridin-4(1H)ones can interact selectively with the iron metal to form a complexation between quinolinic nitrogen-10 with iron(III) and iron(II), which is the metal atom that is close to the N-arene ring. It opens the door to a tentative half-sandwich complex as illustrated in Figure 1E. Recently, we found that 5k showed a selective quenching with the cesium cation, with an apparent dominant interaction on the methoxy moiety.[54] Finally, noncoordinative 2-arylquinazolin-4(3H)-ones were used as a negative control (see structures in Figure S1) and noncomplexation interaction with metals is expected. Then, the ability of these target chemical systems to coordinate with iron$^{2+/3+}$ is essential for its potential application as an inhibitor of β-hematin crystallization within our proposal. The coordination ability of all these heterocyclic systems in conjunction with their good antiparasitic activity against trypanosomatids makes them valuable systems for studying

Table 3. Inhibitory Response against β-Hematin Crystallization (IHC), Toxicity against Murine Peritoneal Macrophages, Selectivity Index (S.I.), Hemolysis Activity, Antimalarial Response for the Infected Model of *P. berghei*, and Partition Coefficient (Log *P*) for the Most Prominent Inhibitors 1d, 1e, 1h, 2a, 2b, 2d, 2e, 2f, 2h, 3b, 3c, 5a, and 5k[a]

Entries	Compds	IC$_{50}$ (μM) ($\pm$ SD), IHP[b]	Toxicity (μM) ($\pm$ SD)[c]	S.I. (CC$_{50}$/IC$_{50}$)[d]	Hemolysis (%) ($\pm$ SD)[e]	%P ($\pm$ SD)[f]	Post-infection days survival ($\pm$ SD)[g]	Log P[h]
1	**1d**	11.34 ± 2.62	> 120	>10.6	11.11 ± 0.06%	34.75 ± 0.170	15.75 ± 0.57	4.00
2	**1e**	13.99 ± 2.40	29.43 ± 1.34	2.1	N.D.	N.D.	N.D.	3.86
3	**1h**	14.06 ± 2.21	45.54 ± 2.56	3.2	N.D.	N.D.	N.D.	3.86
4	**2a**	7.24 ± 0.03	40.00 ± 2.24	5.5	23.54% ± 0.14	1.200 ± 0.097	24.78 ± 0.43	4.01
5	**2b**	7.10 ± 0.02	31.56 ± 2.99	4.5	19.14 % ± 0.15	0.780 ± 0.040	26.15 ± 0.12	4.58
6	**2d**	**5.80 ± 0.04**	56.32 ± 4.01	9.7	26.50 % ± 0.23	**0.230 ± 0.012**	**29.83 ± 0.32**	2.56
7	**2e**	**5.30 ± 0.02**	42.51 ± 3.02	8.0	**21.15 % ± 0.28**	0.410 ± 0.032	**28.07 ± 0.25**	3.13
8	**2f**	**5.50 ± 0.01**	**111.45 ± 6.75**	20.3	**22.13 % ± 0.18**	0.320 ± 0.053	**28.16 ± 0.16**	2.69
9	**2h**	8.51 ± 0.07	25.16 ± 1.63	3.0	35.42% ± 0.21	N.D.	N.D.	1.74
10	**3b**	17.66 ± 0.04	111.21±7.89	6.3	N.D.	N.D.	N.D.	2.97
11	**3c**	15.60 ± 0.04	103.34 ± 9.32	6.6	N.D.	28.25 ± 0.213	16.22 ± 0.72	3.07
12	**5a**	9.70 ± 0.02	67.54 ± 4.86	7.0	N.D.	27.56 ± 0.240	14.23 ± 0.68	4.36
13	**5k**	11.80± 0.02	40.53 ± 1.87	3.4	N.D.	N.D.	N.D.	4.70
14	**C (-)**[i]	-----------	------------	-----------	-----------	78.70 ± 0.092	8.80 ± 0.58	-------
15	**CQ**[j]	1.48 ± 0.01	> 98.48	> 66.5	28.73 % ± 0.12	0.200 ± 0.070	29.98 ± 0.20	-------

[a]Results are expressed as the media ± standard deviation (SD). [b]IHC: inhibition heme crystallization, expressed as IC$_{50}$, for the most active derivatives. [c]Relative toxicity was determined on murine peritoneal macrophages. [d]Selectivity index (S.I.) from IC$_{50}$ of inhibition toward β-hematin and CC$_{50}$ (S.I. = IC$_{50}$/CC$_{50}$). [e]Relative hemolysis percent response was determined on red blood cells at 100 mM. Further hemolysis response data at 1 and 10 mM drug compound concentrations are listed in Table S1. [f]*In vivo* % P: percentage of parasitemia (compound dosage for *in vivo* assay was 20 mg kg^{-1}). [g]Post-infection days determined by using infected mice with *P. berghei*, n = 6 (number of treated mice). [h]Calculated from the SwissADME software website, ref 61. *P < 0.05 compared to the control-treated group. **P < 0.01 compared to the control-treated group. [i]Control negative [C(−)] represents the experiment in the absence of any compound or reference drug. [j]Positive control treated with chloroquine (CQ) (20 mg kg^{-1}).

their inhibitory activity on β-hematin crystallization and antimalarial response against the *Plasmodium* parasite.

***In Vitro* Studies on the Heme Crystallization.** Initially, we focused on the ability of the 66 compounds to inhibit β-hematin crystallization by using the reported method with a few modifications (Tables 1 and 2).[55−57] All these compounds were previously prepared and characterized by our group.[27−33,58,59] From the 4-chloro-1-phthalazine-aryl/hetero-arylhydrazinyl derivatives, four of them (1a, 1d, 1e, and 1h) displayed moderate inhibitory responses with IC$_{50}$ values ranging from 11.34 to 15.93 μM. Phthalazines 1f and 1k exhibited modest inhibitory responses of IC$_{50}$ = 28.79 and 28.80 μM, respectively, whereas the rest of phthalazine-hydrazones including those constructed from acetophenone, i.e., 1n−1t, displayed poor inhibitory responses (IC$_{50}$ > 50 μM). In particular, the non-inhibitory activity of nitro-derivatives 1j, 1l, and 1m can be attributed to its poor solubility in aqueous solution, whereas the non-activity of the phthalazine featuring 2-hydroxyphenyl 1i may be associated with the Z-isometry of the ylidenic bond. It is important to mention that geometric configuration is modestly able to form stable complexes with transition metals. The rest of 1-arylhydrazinyl-phthalazines 1a−1m presented an *E*-isometry. Regarding monosubstituted phthalazines 1n−1t, their modest inhibitory responses can be attributed to their restricted ability

to form a stable complex with metals. Details are discussed later.

Talking about the disubstituted phthalazin-hydrazones (2a−2h), these compounds exhibited the most significant inhibitory activity on the heme crystallization, finding good inhibitory activities for six derivatives (2a, 2b, 2d, 2e, 2f, and 2h) with IC$_{50}$ values ranging from 5.30 to 8.51 μM. That inhibitory response is barely comparable to that found for the chloroquine reference (IC$_{50}$ = 1.22 μM) (Table 2). In particular, the hexadentate 1,4-disubstituted phthalazines 2e (IC$_{50}$ = 5.30 μM) and 2f (IC$_{50}$ = 5.50 μM) displayed the highest inhibitory response within the 1,4-disubstituted phthalazines (Figure 1A), followed by compounds 2d (IC$_{50}$ = 5.80 μM), 2b (IC$_{50}$ = 7.10 μM), 2a (IC$_{50}$ = 7.24 μM), and 2h (IC$_{50}$ = 8.51 μM). The non-inhibitory activity found for nitro-derivatives 2c and 2g seems to be associated with their poor solubility in aqueous solution.

Regarding the 1,2,4-triazolophthalazine system (3a−3f), only two of them, in particular, those bearing *N*-methylpiperazine substitution at the 6-position, 3b and 3c, exhibited moderate responses with IC$_{50}$ values of 15.60 and 17.66 μM, respectively (Table 2). The replacement of the *N'*-methyl-piperazine substitution by a chlorine atom at the 6-position of phthalazine-1,2,4-triazolo led to a reduction of the inhibitory activity (3a in Table 2). These findings suggests that *N'*-methylpiperazine seems to play an important role in the

inhibitory response of the phthalazine-1,2,4-triazolo system. As was mentioned earlier, we demonstrated that this type of system bearing N-methylpiperazine acts as a potassium channel blocker, suggesting its ability to interact with metals.[52] Meanwhile, N^1-aryl-benzo[b]naphthyridin-4(1H)-ones showed a moderate inhibitory response toward heme crystallization, identifying two compounds, **5a** and **5k**, with good IC$_{50}$ values of 9.7 and 11.8 μM, respectively (Table 2). The rest of studied N^1-aryl-benzo[b]naphthyridin-4(1H)-ones showed comparable inhibitory responses to each other with IHP values from 26 to 39% at a 50 μM drug concentration. It seems clear that the 8- or 7-methoxy substitution on the benzo-core plays an important role in the inhibitory activity of these interesting compounds because the majority of their derivatives (**5a**, **5b**, **5j**, or **5 k**) presented IHP values higher than 35% (with a few exceptions). The nonsubstituted derivatives (**5g**) or methyl-substituted derivatives (**5d**, **5f**, and **5i**) showed more discrete IHP responses from 9 to 26%. It is important to mention that the 7-methoxy derivatives (**3j**, **3k**, and **3l**) were consistently more active than 7-methoxy derivatives, which suggested that the disposition of the methoxy group at the 7-position of the benzo-core seems to be relevant in the inhibition of β-hematin crystallization. Recently, we found that the 7-methoxy derivatives showed more efficient π–π stacking between two molecules of benzo[b]naphthyridin-4(1H)-one than 8-methoxy derivatives from X-ray crystal structure packing (Figure S2), which was associated with a homogeneous distribution of Mulliken charge along the benzo[b]naphthyridin-4(1H)-one ring (Figure S3). It may play an important role in the inhibition of β-hematin through π–π stacking between benzo[b]naphthyridin-4(1H)-one and one porphyrin molecule as has been described for 4-aminoquinolines. It is important to mention that the direct interaction of the quinolinic nitrogen-10 of the ligand with the iron(III) metal is drastically compromised by the presence of vicinal N^1-arene, which is more remarkable by the hindrance environment of the iron(III) metal into the heme group. As a comparative reference, some analogues of our N^1-aryl-benzo[b]-naphthyridin-4(1H)one such as the floxarcrine or chromones containing a trifluoromethyl moiety have demonstrated good inhibitory responses toward the heme crystallization, which put in evidence of the role of the quinolin-4(1H)one ring for the design of β-hematin inhibitors.[25]

Finally, as we expected, none of the noncoordinative 2-arylquinazolin-4(3H)-ones **4a**–**4u** presented inhibitory responses at a drug concentration of 50 μM. All these findings reflect that the coordinative character of the tested molecules seems to play a pivotal role in the inhibitory response toward heme crystallization, finding the highest response for highly coordinative 1,4-disubstituted phthalazine derivatives **2a**–**2h**, followed by a moderate coordinating system like monosubstituted phthalazines **1a**–**1t**, 1,2,4-triazolophthalazines **3b** and **3c**, and N^1-aryl-benzo[b]naphthyridin-4(1H)ones **5a**–**5l**, and a non-inhibitory response for the noncoordinative 2-arylquinazolin-4(3H)-ones **4a**–**4u**.

***In Vitro* Toxicity Assay.** The toxicity assay was performed for the most prominent inhibitors **1d**, **1e**, **1h**, **2a**, **2b**, **2d**, **2e**, **2f**, **2h**, **3b**, **3c**, **5a**, and **5k** by using peritoneal murine macrophages. The latter were obtained from the mouse peritoneal cavity.[30–33] Toxicity results (expressed in terms of CC$_{50}$) are summarized in Table 3. Among the studied compounds, **1d**, **3b**, **3c**, and **2f** exhibited the lowest toxicity against macrophage cells with CC$_{50}$ values higher than 100

μM, followed by the N^1-aryl-benzo[b]naphthyridin-4(1H)ones **5a** and **5k** with CC$_{50}$ values of 67.54 and 40.53 μM, respectively, the 1,4-disubstituted phthalazines **2a**–**2f** with CC$_{50}$ values from 31.56 to 56.32 μM, and the monosubstituted phthalazines **1e** and **1h** with CC$_{50}$ values of 29.43 and 45.54 μM, respectively. Finally, the nitro-derivative **2h** showed the highest toxicity with a CC$_{50}$ value of 25.16 μM. Toxicity results were matched with their corresponding IHC (inhibition of β-hematin crystallization) response to obtain a relative selectivity index (S.I.), which was used as a criterion to select the best candidate for *in vivo* efficacy studies. Consequently, only the best candidate with the highest S.I. from each compound group was selected for further assays. Then, compound **1d** (S.I. > 10.6) was chosen from group 1 over compounds **1e** (S.I. = 2.1) and **1h** (S.I. = 3.2). From group 2, compounds **2f** (S.I. = 20.3), **2d** (S.I. = 9.7), **2e** (S.I. = 8.0), and **2a** (S.I. = 5.5) were selected as the best candidates. Derivative **2b**, despite its modest S.I. (4.5), was chosen for further assays, taking advantage of its potential as a leishmanicidal agent against infective strains of the *Leishmania* parasite.[30] Within group 3, despite the similar inhibitory or cytotoxicity response found between compounds **3b** and **3c**, **3c** was chosen for further assay based on its recognized antiparasitic activity. Previously, we demonstrated the potential of **3c** as a leishmanicidal agent with significant *in vitro* activity against the infective and resistant strain of the *Leishmania* parasite, which was higher than that found for derivative **3b**.[31] Finally, compound **5a** (S.I. = 7.0) was chosen over **5k** (S.I. = 3.4) from group 5.

***In Vitro* Hemolysis Assay.** To discard any potential toxic effect on red blood cells (RBCs) by the highly coordinative ability of the tested compounds, we performed hemolysis assays using human red blood cells (RBCs) for the most active compounds **1d**, **2a**, **2b**, **2d**–**2f**, and **2h**. It is significantly relevant for the most active disubstituted phthalazines (**2a**–**2h**) because they justly can easily form a complex with metallic species[39–42] including the iron present in red blood cells (RBCs) and other metabolic enzymes like cytochrome family enzymes. An assay was performed at three compound concentrations (1, 10, and 100 mM). The hemolysis data are listed in Table 3, and further information details can be found in Table S1. From the results, it should be noted that all active disubstituted phthalazines **2a**, **2b**, **2d**, **2e**, **2f**, and **2h** displayed a discrete hemolysis (19–35%) response at a high compound concentration (100 mM), which was in general comparable to that response found for the CQ (28.73%). In particular, derivative **2b** disclosed the lowest hemolysis activity, whereas the nitro-derivative **2h** displayed the highest response, which was in good correlation with its relative *in vitro* toxicity against macrophages. The latter compromises the applicability of derivative **2h** as an antimalarial agent. At a 1 mM compound concentration, low hemolysis activity from 5.20 to 12.40% was found for the 1,4-disubstituted derivatives, having the lowest hemolysis for compound **2b** and the highest for compound **2h**. Candidate derivatives **2d** and **2f** displayed hemolysis response values of 8.70 and 9.2% at a 1 mM compound concentration, respectively, which were comparable to that found for the chloroquine reference (7.40%) (Table S1). Meanwhile, derivative **1d** showed a lower hemolysis (11.1%) response than 1,4-disubstituted aryl-hydrazinyl-phthalazines **2a**–**2h** (19–35%) at a 100 mM compound concentration. From the hemolysis assay, most of tested 1,4-disubstituted aryl-hydrazinyl-phthalazines **2a**–**2h** as well as compound **1d** were considered safe against RBCs for further biological assays.
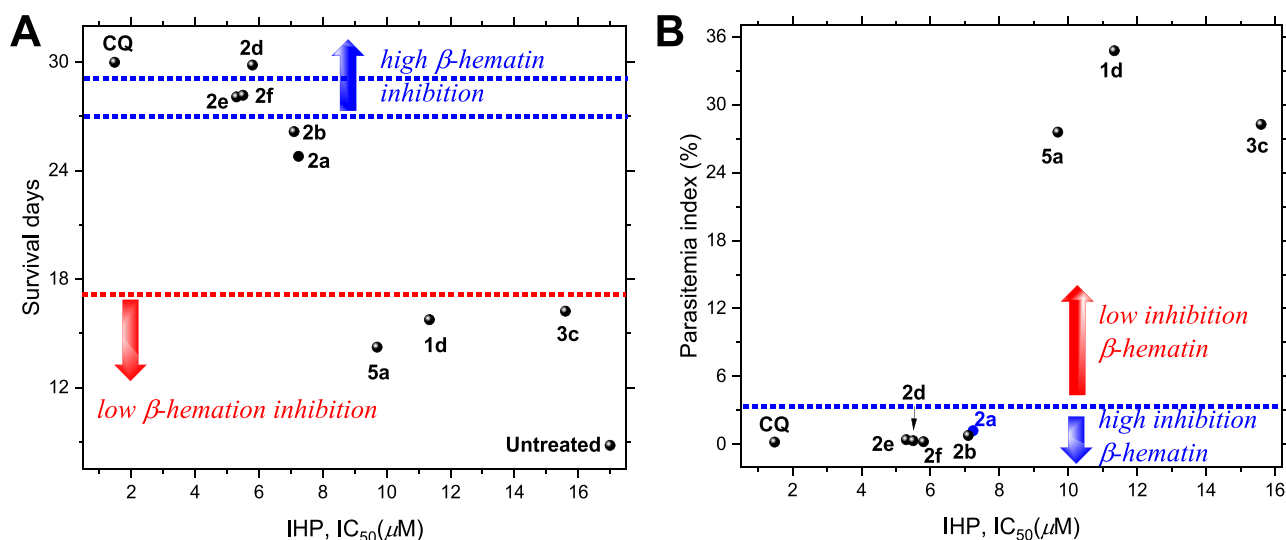
Figure 2. Correlation between the inhibitory response toward β-hematin and survival days post infection (A) and parasitemia index (B) for the most active compounds.

***In Vivo* Efficacy.** A selected group of compounds with low toxicity and good inhibitory response against β-hematin crystallization were tested *in vivo* in the *P. berghei*-infected model. The selected compounds consist of a series of compounds with S.I. higher than 5 and low hemolysis response including (i) the best β-hematin inhibitors of 1,4-disubstituted phthalazines (**2a**, **2b**, **2d**, **2e**, and **2f**) and (ii) moderate and nontoxic inhibitors of 1-substituted phthalazine-hydrazone (**1d**), 1,2,4-triazolophthalazine (**3c**), and N^1-aryl 2-trifluoromethyl-benzo[*b*]naphthyridin-4(1*H*)-ones (**5a**). The *in vivo* model consisted of mice infected with *P. berghei* ANKA, a chloroquine-susceptible strain of murine malaria (Table 1). Efficacy in the *P. berghei* assay was determined following oral administration of 20 mg kg^{-1} day^{-1} for 4 consecutive days (4 day Peters' test). The parasitemia was determined at 4 day post-infection, and subsequently, the survival days for treated mice with compounds were monitored and compared with negative untreated mice for symptoms for up to 30 days.[60] Experimental details can be found in the Experimental Section and Supporting Information. The efficacy results are summarized in Table 1. The untreated mice died between 7 and 8 days post infection, whereas treated mice displayed a superior survival time in conjunction with a diminution of parasitemia. In general, all tested compounds were able to increase the survival time post infection in conjunction with a reduction of the parasitemia compared to the untreated control (9 survival days and parasitemia index by about 79%). Within the tested compounds, 1,4-disubstituted phthalazine-hydrazones (**2**) were able to enhance the survival time over 20 days post infection (average mice survival days from 24 to 28 days) with a significant reduction of parasitemia, having the lowest parasitemia percentages in treated mice from 0.23 to 1.14% (parasitemia reduction percentage from 99.77 to 98.86%). From the 1,4-disubstituted phthalazines, two of them (**2d** and **2f**) afforded a complete cure (3/3 mice cured and survival days of 30) with parasitemia reduction by about 99.77 and 99.68%, respectively, at day 4. The efficacy of the most active 1,4-disubstituted phthalazines (**2d**, **2e**, and **2f**) was comparable to that found for the chloroquine reference with a parasitemia index of 0.2% (3/3 mice with parasitemia reduction of 99.80%) and a survival time of >30 days, making these 1,4-disubstituted

phthalazines potential antimalarial agents targeting the inhibition of β-hematin crystallization. Meanwhile, the rest of derivatives (no 1,4-disusbtituted phthalazines) displayed modest antimalarial activity with a survival time from 14 to 16 days and a parasitemia percentage in infected mice of about 27−29% post infection. Interestingly, neither of the structural analogues of the 1,4-disubstituted phthalazines, the monosubstituted phthalazines **1d** and the cyclic version **3c**, were efficacious at 20 mg/kg drug dosage, which suggests that the 1,4-disusbtitution is pivotal in the antimalarial activity of the studied phthalazines.

In general, a good correlation between the activity against the *P. berghei* model and the inhibitory activity against β-hematin crystallization was found for the studied derivatives, suggesting that the inhibition of heme crystallization is the main mode of action of these most active compounds, in particular, for the 1,4-disubstituted phthalazine-hydrazones. A general correlation between the inhibitory activity and the parasitemia index and survival times is shown in Figure 2, which illustrates clearly the important role of the inhibition of β-hematin in promoting a high curative response with reduction of parasitemia (Figure 2A,B). From Figure 2, the best inhibitors **2d**, **2e**, and **2f** displayed a high curative response and reduction of parasitemia, close to that found for CQ, whereas modest inhibitors **1d**, **3c**, and **5k** exhibited the lowest curative and antiparasitic response.

In definition, a comparison between *in vitro* β-hematin inhibition, antimalarial activity (survival time and parasitemia), hemolysis, toxicity, and Log *P* reflects that derivatives **2d** and **2f** emerged as the most promising agents with a good inhibitory response toward heme crystallization (IC$_{50}$'s of 5.80 and 5.50 μM for compounds **2d** and **2f**, respectively), moderate toxicities (CC$_{50}$'s of 56.32 and 111.45 μM for compounds **2d** and **2f**, respectively), hemolysis (less than 22%), post-infection day survival (28−29 days), parasitemia indexes (0.230 and 0.320 for compounds **2d** and **2f**, respectively), and partition coefficient (Log *P* < 3). Compound **2e** showed an interesting profile, but it showed higher toxicity (CC$_{50}$ = 42.51 μM), barely higher parasitemia index for treated mice (0.410), and partition coefficient (Log *P* = 3.13).

Table 4. *In Silico* Physicochemical, Pharmacokinetic, and Druglikeness Parameters of the Prominent Antimalarial Candidates 2d and 2f

type of parameter	parameter	2d	2f
physicochemical properties	MW (g/mol)[a]	456.41	346.34
	no. of rotatable bonds	8	6
	no. of H-bond acceptors	8	6
	no. of H-bond donors	2	2
	molar refractivity	132.14	99.03
	TPSA (Å^2)[b]	166.20	100.84
delipophilicity	Log $P_{o/w}$ (iLOGP)	1.49	1.56
	Log $P_{o/w}$ (XLOGP3)	4.65	3.79
	Log $P_{o/w}$ (WLOGP)	3.96	3.33
	Log $P_{o/w}$ (MLOGP)	2.90	1.88
	Log $P_{o/w}$ (SILICOS-IT)	−0.17	2.92
	Consensus Log $P_{o/w}$	2.56	2.69
water solubility	Log S (ESOL)	−5.55	−4.55
	solubility	2.82 μM (moderately soluble)	28.3 μM (moderately soluble)
	Log S (Ali)	−7.87	−5.60
	solubility	13.6 nM (poorly soluble)	2.50 μM (moderately soluble)
pharmakinetic properties	G.I. absorption[c]	low	high
	BBB permeant[d]	no	no
	P-gp substrate[e]	no	no
	CYP1A2 inhibitor	no	yes
	CYP2C19 inhibitor	yes	yes
	CYP2C9 inhibitor	yes	no
	CYP2D6 inhibitor	no	no
	CYP3A4 inhibitor	yes	no
	Log K_p (skin permeation)	−5.78 cm/s	−5.72 cm/s
druglikeness	Lipinski	yes; 1 violation: NorO > 10	yes; 0 violation
	Ghose	no; 1 violation: MR > 130	yes
	Veber	no; 1 violation: TPSA > 140	yes
	Egan	no; 1 violation: TPSA > 132	yes
	Muegge	no; 1 violation: TPSA > 150	yes
	bioavailability score	0.55	0.55
medicinal chemistry	PAINS[f]	0 alert	0 alert
	Brenk	2 alerts: imine_1, nitro_group	1 alert: imine_1
	leadlikeness	no; 3 violations: MW > 350, Rotors > 7, XLOGP3 > 3.5	no; 1 violation: XLOGP3 > 3.5

[a]MW: molecular weight. [b]TPSA: topological polar surface area. [c]G.I.: gastrointestinal. [d]BBB: blood−brain barrier. [e]P-gp: P-glycoprotein. [f]PAINS: pan assay interference structure. The rest of *in silico* data can be found in Tables S1−S5 of the Supporting Information. Fundamental definition of each parameter can be found in ref 62.

***In Silico* ADME Parameters.**[62] In an attempt to rationalize the varying *in vivo* efficacies, an *in silico* analysis of the physicochemical, pharmacokinetic, and druglikeness parameters through the SwissADME website[61] was performed for the best candidates of each compound family (Table 2 and Tables S1−S4 in the Supporting Information). Focusing on three more active derivatives **2d**, **2e**, and **2f**, compound **2f** showed the best profile with (i) the best water solubility, about 10-fold more than those of derivatives **2d** and **2e**, (ii) higher gastrointestinal (G.I.) absorption, (iii) a lower inhibitory activity toward cytochrome proteins, exhibiting only a tentative activity on CYP1A2 and CYP2C19 proteins, (iv) no violations of druglikeness principles, and (v) the absence of a PAINS (pan assay interference structure) moiety. Derivative **2e** seems to be the least convenient candidate because it presents a PAINS moiety such as the hydrizinyl-phenol ring as well as the violation of two lead-likeness principles (MW > 350, XLOGP3 > 3.5). Meanwhile, despite the different drawbacks found for compound **2d** including (i) the violation of three lead-likeness principles (MW > 350, Rotors > 7, XLOGP3 > 3.5) and (ii) two alerts within Brenk's ruler (imine and nitro groups) and

large TPSA (166.20 Å^2), these compounds showed the best survival time for treated mice and a lower parasitemia index post infection, which are comparable to the CQ reference. The latter reflects that the tentative side effects and solubility limitation would not seem to be dominating for the *in vivo* model, thus being a candidate to be taken into account for further assays. From the results, it should be noted that compounds **2d** and **2f** with a better ADME profile showed the most significant *in vivo* antimalarial response (Table 4). The discrete antimalarial activity and curative properties of derivatives **2a**, **2b**, and **2h** can be associated with the higher Log P of derivatives **2a** and **2b** and lower water solubility of **2h** (details in Tables S1−S4). Meanwhile, despite the good ADME profile and good simulated pharmacokinetic properties and druglikeness found for derivatives **1d** and **3c**, their low *in vivo* efficacy may be mainly attributed to the lack of an intrinsic biological activity of them against the *Plasmodium* parasite (Table S4). Also, finally, the N^1-(aryl)-2-(trifluoromethyl)-8-methoxybenzo[*b*][1,8]naphthyridin-4(1*H*)-ones **5a** and **5k** showed a good ADME, pharmacokinetic, and druglikeness profile from the *in silico* study, although they exhibited a low
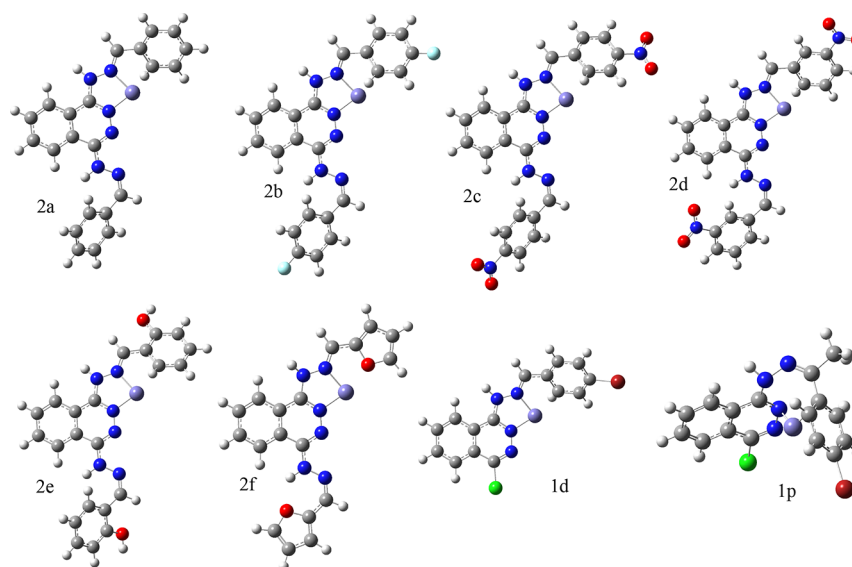
Figure 3. Structure of ligand−iron(III) complexes for the disubstituted phthalazin-hydrazones **2a−2f** and monosubstituted phthalazin-hydrazones **1d** and **1p**.
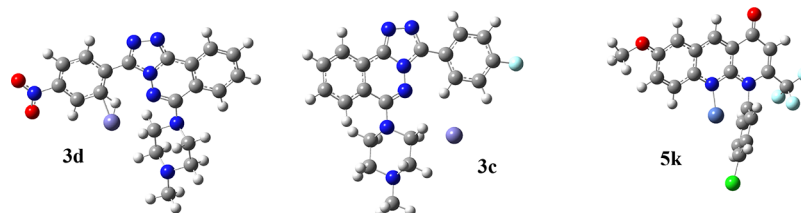
Figure 4. Structure of ligand−iron(III) complexes for the 3-aryl-6-(N'-methylpiperazine)-1,2,4-triazolophthalazines **3c** and **3d** and N^1-aryl 2-trifluoromethyl-benzo[b]naphthyridin-4(1H)-one **5k**.

Table 5. Comparison between the Complexation Ability and TPSA Data of the Most Active Derivatives with Its Inhibitory Response toward β-Hematin Crystallization

Entries	Compounds	$K_a \times 10^7$ (M^{-1})	$E_{Complx\,(Fe^{2+})}{}^a$	$E_{Complx\,(Fe^{3+})}{}^b$	TPSA (Å²)ᶜ	IC$_{50}$ (μM) (± SD)ᵈ
1	**1d**	0.032	**-359.29**	-800.50	50.17	11.34 ± 2.62
2	**1p**	N.D.	-328.05	N.C.	49.11	>50.0
3	**2a**	1360	**-358.45**	**-886.26**	74.56	7.24 ± 0.03
4	**2b**	1250	**-352.30**	**-880.21**	74.56	7.10 ± 0.02
5	**2c**	150	-241.06	-850.33	166.20	>50.0
6	**2d**	3100	-337.92	-853.76	166.20	**5.80 ± 0.04**
7	**2e**	2200	-365.06	-872.45	115.02	**5.30 ± 0.02**
8	**2f**	1510	**-394.77**	**-920.19**	100.84	**5.50 ± 0.01**
9	**2h**	550	**-374.07**	-827.15	192.48	8.51 ± 0.07
10	**3a**	N.D.	-258.40	-686.08	40.32	>50.0
11	**3c**	>0.0001	-308.56	N.C.	49.56	15.60 ± 0.04
12	**3d**	>0.0001	N.C.	N.C.	98.61	>50.0
13	**4b**	~ 0.00	N.C.	N.C.	41.46	>50.0
14	**5k**	0.0003	-263.39	-729.17	44.12	11.80
15	**CQ**	0.063	N.D.		27.63	1.48

^{a}Complexation energy between the ligand and iron(II) calculated from B3LYP/6.31G(d,p). ^{b}Complexation energy between the ligand and iron(III) calculated from B3LYP/6.31G(d,p). ^{c}TPSA (topological polar surface area) calculated from SwissADME. ^{d}IC$_{50}$ for the inhibition heme crystallization. Red color, critical case; bold black text, highlighted results. N.D., not determined.

aqueous solubility. It may be one of the main physicochemical factors that affect the *in vivo* efficacy of these compounds, although the lack of intrinsic antiparasitic activity cannot be discarded.

Role of the Complexation with the Iron Metal. To confirm the role of the complexation ability of the ligand in the inhibition of β-hematin crystallization, we studied the ability of the most active derivative to form a complex with the iron(III) ion from theoretical and experimental studies. Iron(III) is the main oxidation state present in the iron atom featuring the β-hematin crystal. Extra complexation calculations of the ligands were performed for iron(II) ions to explore the relative coordinative selectivity of the ligand because iron(II) is present in important human enzymes, cytochrome, hemoglobins, etc. Regarding theoretical calculations, first, the geometries of the studied derivatives were optimized by using the B3LYP method[63] in combination with the 6-31G(d,p) basis set.[64] The calculations were implemented in Gaussian09 package
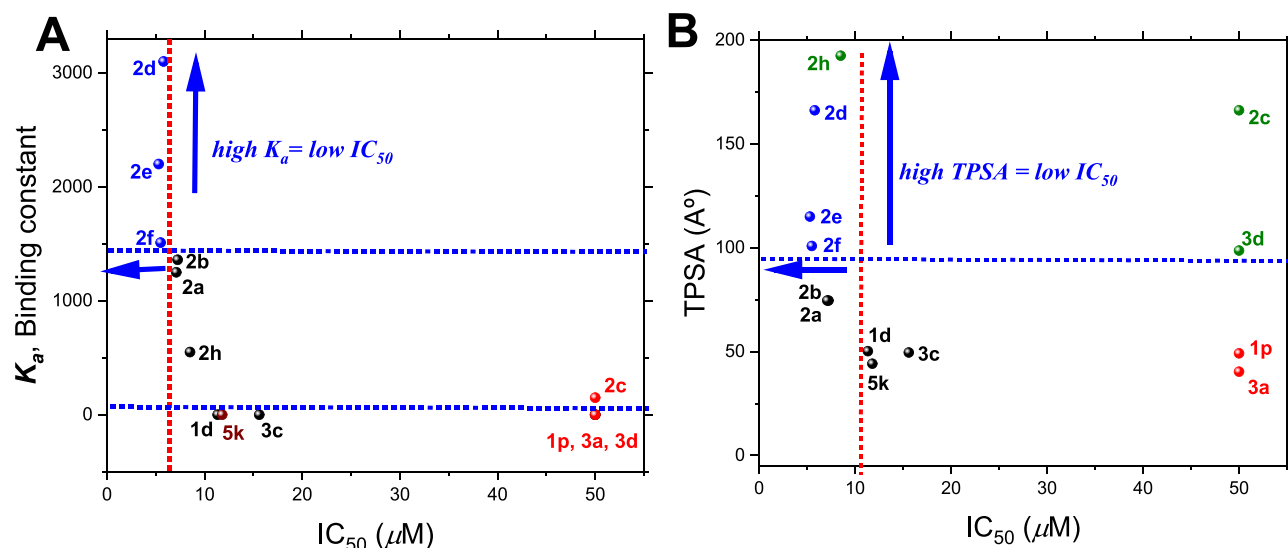
Figure 5. Correlations between the inhibitory response toward β-hematin crystallization and the binding constant of the ligand−iron(III) complexation (A) and the TPSA of the ligand (B). Blue points remark the most promising compounds, red points indicate the less prominent correlation, and green points are taken as exceptions to the general correlations.

software.[65] Subsequently, the interaction between the most active ligand and a molecule of iron(III) or iron(II) was performed by using the BSSE model-implemented counterpoise command.[66] All optimized ligand and complex structures can be found in Section VI of the Supporting Information. Some relevant structures and complexation energies are summarized in Figures 3 and 4 and Table 5, respectively. From the results, the disubstituted phthalazines (group 2), in general, showed the highest complexation ability among the studied compounds with complexation energies from −827 to −920 kcal/mol. Within group 2, nitro-derivatives **2c**, **2d**, or **2h** showed the lowest complexation ability with complexation energies of −850.33, −853.76, and −827.15 kcal/mol, respectively, whereas compound **2f** displayed the highest complexation energy (−920.19 kcal/mol). Meanwhile, the monosubstituted phthalazine **1d** showed a complexation energy of −800 kcal/mol, which was comparable to those found for the disubstituted 1,4-arylhydrazinyl-phthalazines (−827 to −927 kcal/mol). It is expected because the complexation calculations for disubstituted phthalazines were performed by using one molecule of iron(III), although the higher complexation energies of disubstituted phthalazines suppose that they present a higher complexation ability than monosubstituted phthalazines. The 3-aryl-1,2,4-triazolophthalazines **3c** displayed a complexation energy of −686.1 kcal/mol, whereas the trifluoromethyl-benzo[*b*]naphthyridin-4(1*H*)-one **3k** showed a complexation energy of −301.1 kcal/mol. The rest of derivatives **1p**, **3a**, and **3d** did not show convergence of the geometry of their corresponding iron complexes, putting in evidence of the poor ability of these compounds to form stable complexes with iron(III). For derivative **1p**, the incorporation of the methyl group on the ylidenic bond seems to affect the coordination character of the ligand because the aryl ring tends to place in the coordination region (see **1p** in page S19 of the Supporting Information and Figure 3 for its iron complex). On the other hand, the complexation tendency of the ligands is comparable between iron(III) and iron(II), although the ligand showed a preference toward iron(III) over iron(II) with lower complexation energies (*e.g.*, −800 vs −350 kcal/mol for 1,4-diarylhydrazi-

nylphthalazines). It has great relevance because a high complexation preference toward iron(II) could more selectively favor the inhibition of β-hematin formation than the interaction with any essential iron enzyme or protein rich in iron(III).

Experimental determination of complexation confirmed the theoretical findings (Table 5). In general, the 1,4-arylhydrazinyl-phthalazines disclosed the highest binding constants with values from 550×10^7 to 3100×10^7 M^{-2}. The 1,4-diarylhydrazinyl-phthalazines showed a stoichiometry ratio of 2, whereas the rest of ligands showed a stoichiometry ratio of 1. Within the highly coordinative 1,4-arylhydrazinyl-phthalazines, the highly conjugated nitro-derivatives **2c** and **2h** showed the lowest binding constants of 150×10^7 and 550×10^7, respectively, whereas **2d** and **2f** exhibited the highest affinity complexation with values of 3100×10^7 and 1510×10^7 M^{-2}, respectively. Regarding the rest of ligands, the monosubstituted 1-arylhydrazinyl-phthalazine **1d** displayed a lower binding constant of 3200 M^{-1} and derivative **5k** displayed a binding constant of 30 M^{-1}, whereas the 1,2,4-triazolophthalazines displayed the lowest complexation ability with a binding constant of less than 10 M^{-1} for compounds **3c** and **3d**. The CQ showed a discrete binding constant of about 6300 M^{-1}, which suggests that the inhibitory response is not strictly dependent on its complexation ability toward the iron(III) metal, but also other chemical functionality may play an important role. It is documented that the terminal tertiary amine moiety is interacting with the terminal carboxylate group of the porphyry ring of the heme group, thus with the presence of the alkyl group relevant for a high inhibition of the β-hematin formation.[7]

Regarding the nature of complexes, as expected, the mono- or di-arylhydrazinyl-phthalazines (groups 1 and 2) are able to coordinate with the iron metal through imine nitrogen and nitrogen-2 of the pyrazine ring to form a five-membered cycle (Figure 3) with complexation energies of less than −800 kcal/mol and a binding constant of 3200 for monosubstituted compounds and in the 10^8 range for disubstituted phthalazines. Meanwhile, the triazolophthalazine ligands bearing *N'*-methylpiperazine showed the iron(III) metal placed close to

the piperazine ring, but it is not sufficient to form a stable complex (no convergence of complex geometry) (Figure 4), whereas the N^1-aryl 2-trifluoromethyl-benzo[*b*]naphthyridin-4(1*H*)-one coordinates through quinolinic nitrogen-10 and a vicinal arene ring to form a classical half-sandwich complex and that mode of coordination allows one to interpret the high complexation ability of the rigid benzo[*b*]naphthyridin-4(1*H*)-one (**5k** in Figure 3). It is important because the complexation character of the ligand plays an important role in the inhibition of β-hematin crystallization via retention of the iron metal. From calculation and experimental studies, the least coordinative ligands, the 1,2,4-triazolophthalazines **3a**, **3c**, and **3d**, showed the lowest inhibition response, whereas the highest coordinative ligands, the phthalazine-hydrazones (groups 1 and 2), displayed the highest inhibition response from 5 to 10 μM. In particular, the double coordinative character of the disubstituted ligand to form dinuclear complexes may favor the ability of these compounds to interact more efficiently with the iron metal than the monosubstituted ligand, which can help interpret the highest inhibitory response of disubstituted phthalazine (5 μM) compared to monosubstituted phthalazine (>10 μM) (Tables 1 and 2). A weak coordinative ligand such as phthalazine-hydrazone **1p** showed a non-inhibitory response. A weak ligand by incorporation of strong electron-deficient nitro-rings compromises an effective complexation, which was transduced in a weak inhibitory response (*e.g.*, **2c**, **2g**, and **2h**). Regarding the N^1-aryl 2-trifluoromethyl-benzo[*b*]naphthyridin-4(1*H*)-one, the proximity of the *N*-arene moiety to the structure may compromise the ability of the ligand to interact directly with the iron metal of the heme group, which is reflected in its lower binding constant of about 29 M^{-1}. That lower binding constant may be correlated with the moderate inhibitory response (IC_{50} values of more than 9 μM) of the N^1-aryl 2-trifluoromethyl-benzo[*b*]naphthyridin-4(1*H*)-ones **5a** and **5k**. To establish a more consistent correlation between the inhibitory response and the complexation ability and surface extension of the ligand, we constructed K_a *vs* IC_{50}. The graphical representation is illustrated in Figure 5A. From Figure 5A, the ligands with higher binding constants, **2d**, **2e**, and **2f**, showed the most significant inhibitory response, whereas the less coordinative ligands **1p**, **3a**, and **3d** did not a show inhibitory response. The inhibitory response showed a direct and consistent correlation with the complexation ability of the ligand to coordinate with iron(III), and the correlation K_a *vs* IC_{50} showed an exponential behavior, where a significantly high complexation character of the ligand guarantees a high inhibitory response toward β-hematin crystallization.

Beyond the role of the complexation ability of the ligand, it should be noted that the extension or surface area of the ligand may be relevant for the inhibition process to favor ligand–hematin interaction via an effective π–π stacking. To clarify that observation, we constructed a TPSA *vs* IC_{50} plot, and the graphic is shown in Figure 5B. From Figure 5B, the most extended compounds with high TPSA (>100 Å) showed the highest inhibitory response, with an exception of the nitro-derivatives. Similar to the K_a *vs* IC_{50} tendency, the TPSA *vs* IC_{50} exhibited a pseudo-exponential behavior, showing a high inhibitory response with an increase in TPSA magnitude. Less extended ligands such as **1p** (49.11 Å) and **3a** (40.32 Å) did not show an inhibitory response, whereas other ligands like **1d** (50.17 Å), **3c** (49.56 Å), and **5k** (44.12 Å) showed a modest

inhibitory response. Then, the location at the left position of the TPSA vs IC_{50} plot for compounds **2d**, **2e**, and **2f** puts in evidence of the important role of the extension of the molecule for a high inhibitory response. The planar molecular disposition and high extension of the surface of the 1,4-disubstituted phthalazine with TPSA values of more than 100 Å (Table 2 and Tables S2–S5) seem to be convenient features to favor the interaction with β-hematin through a π–π stacking with the porphyrin ring. It can favor the rupture of π–π stacking between porphyrin rings into β-hematin. All evidence suggests that the 1,4-disubstituted phthalazines act as an inhibitor of β-hematin, which are unique chemical systems among studied compounds that present high TPSA values and are able to form a stable complex with iron(III). Our results showed that these two features seem to be important to promote high inhibition and they can be essential for the rational design of β-hematin inhibitors. Probably, the inhibition of the β-hematin crystallization initially involves a π–π stacking between the ligand core and the porphyrin ring of the heme group, and the strength of the hematin–ligand interaction is increased by the interaction between the ligand and the iron(III) placed into the heme group. Both interacting events are favored by the high planarity, extension of the molecular system, and its highly coordinative character with two equivalents of possibility to form polynuclear complexes.

■ CONCLUSIONS

In summary, we evaluated the potential of a series of highly coordinative ligands with known leishmanicidal activity for the inhibition of the formation of β-hematin and antimalarial activity against an *in vivo* model of *P. berghei*. In particular, a group of highly coordinative phthalazines bearing coordinative moieties at 1- and 4-positions showed a high inhibitory response against the formation of β-hematin as well as low toxicity on macrophages and low hemolysis response on human RBCs. Two of the 1,4-disubstituted phthalazines (**2d** and **2f**) disclosed a good curative response and significant reduction of parasitemia from the *in vivo* model of *P. berghei*, with all these findings comparable to those found for the CQ reference. Compound **2f** displayed the best toxicity and ADME profiles, which is a promising candidate for further biological experiments including *in vitro* assay against CQ-sensitive and CQ-resistant *Plasmodium falciparum* models, genotoxicity evaluation, pharmacokinetic studies, and *in vivo* assays.

The significant inhibitory response for the formation of β-hematin seems to be associated with the complexation ability of the active ligands with iron(II) and iron(III) metals. A consistent correlation between the complexation ability of the ligand and the inhibitory response toward β-hematin crystallization was found for a group of active compounds, having the highest inhibitory response for the best ligands with the highest binding constants with iron(III). Alternatively, a good correlation between the TPSA and the inhibitory response of the ligand was found, finding a high inhibition response for ligands with high TPSA values. The present investigation opens new perspectives toward the rational design of antimalarial agents targeting β-hematin crystallization, which is the highly coordinative character of the ligand to form a stable complex with iron(III) and its high molecular surface with planar disposition, two relevant features to take into account for future design of β-hematin inhibitors.

■ EXPERIMENTAL SECTION

Materials and Instruments. The (E)-1-(2-benzylidene-hydrazineyl)-4-chlorophthalazines **1a**–**1t** (Z-isomer for **2i**), 1,4-bis(2-((E)-benzylidene)hydrazinyl)phthalazines **2a**–**2h**, 3-aryl-6-(N′-methylpiperazine)[1,2,4]triazolo[3,4-a]phthalazines **3a**–**3f**, 2-arylquinazolin-4(3H)-ones **4a**–**4u**, N^1-(aryl)-2-(trifluoromethyl)-8-methoxybenzo[b][1,8]naphthyridin-4(1H)-ones **5a**–**5l** were previously prepared and characterized by our group.[27−33] The chloroquine reference was purchased from Sigma-Aldrich and they were used without further purification for the biological analysis. Solvents (ethanol or DMSO) were purchased from commercial sources (Sigma-Aldrich or Merck). Absorption data for the β-hematin crystallization assay were obtained from a Thermo Scientific Varioskan Flash Multimode instrument for air-equilibrated solutions at 25 °C.

Biological Experimental Information. Peritoneal macrophages were obtained from the mouse peritoneal cavity and differentiated in a conditioned medium (medium RMPI) as described in previous methodologies.[30−33] The macrophages were provided by Instituto de Biomedicina "Dr. Jacinto Convit" (Hospital Vargas, Caracas, Venezuela). The P. berghei ANKA strain and mice for in vivo assay were provided by Instituto de Higiene (Universidad Central de Venezuela, Caracas). Mice (average body weight, 16.7 g) were infected with P. berghei parasites by intraperitoneal (IP) inoculation of donor mouse blood diluted in normal saline to contain 3×10^6 infected red blood cells (RBCs). The BALB/c female mice used in this assay were 4 weeks old and pathogen-free (Instituto de Higiene, Universidad Central de Venezuela, Caracas).

Inhibition of β-Hematin Formation. The β-hematin formation assay was performed according to the literature.[55−57] Briefly, a solution of hemin chloride (50 μL, 4 mM), dissolved in DMSO (5.2 mg mL^{-1}), was distributed in 96-well microplates. Different concentrations (5−100 μM) of quinoline compounds dissolved in DMSO were added in triplicate in test wells (50 μL). Controls contained either water (50 μL) or DMSO (50 μL). β-Hematin formation was initiated by the addition of acetate buffer (100 μL 0.2 M, pH 4.4). Plates were incubated at 37 °C for 48 h to allow completion of the reaction and centrifuged (4000 rpm × 15 min, IEC-CENTRA, MP4R). After discarding the supernatant, the pellet was washed twice with DMSO (200 μL) and finally dissolved in NaOH (200 μL, 0.2 N). The solubilized aggregates were further diluted 1:2 with NaOH (0.1 N) and absorbance was recorded at 405 nm (Microplate Reader, BIORAD-550). The results were expressed as a percentage of inhibition of β-hematin crystallization (% IHC).

Parasite, Experimental Host, and Strain Maintenance. Male BALB/c mice weighing 18−22 g were maintained on a commercial pellet diet and housed under conditions approved by Ethics Committee. P. berghei (ANKA strain), a rodent malarial parasite, was used for infection. Mice were infected by ip injection with 1×10^6 infected erythrocytes diluted in phosphate-buffered saline solution (PBS, 10 mM, pH 7.4, 0.1 mL). Parasitemia was monitored by microscopic examination of Giemsa-stained smears.

Four Day Suppressive Test. BALB/c mice (18−22 g) were infected (using caudal vein) with 10^6 infected RBCs with P. berghei (n = 6). Two hours after infection, treatment began with the best compounds tested resulting from in vitro assays. These compounds were dissolved in DMSO (0.1 M), diluted with saline-Tween 20 solution (2%). Each compound (20 mg kg^{-1}) was administered once by ip for 4 days. At day 4, parasitemia was counted by examination of Giemsa-stained smears. Chloroquine (20 mg kg^{-1}) was used as a positive control. The survival time beyond the control group (saline-treated) was recorded. The results were expressed as a percentage of parasitemia (% of parasitemia) and survival days of each compound-treated group over the control (saline-treated group).[60]

Toxicity Assay. Peritoneal murine macrophages were grown in RPMI 1640 medium (Invitrogen) supplemented with 10% heat-inactivated fetal bovine serum, 1% L-glutamine, 1% streptomycin, and 100 units/mL penicillin (all obtained from Sigma-Aldrich, USA). Cell viability was assessed using 3-(4,5-dimethylthiazol-2-yl)-2,5-diphenyltetrazolium bromide (MTT) for assay, which is based on the ability of viable cells to metabolically reduce a yellow tetrazolium salt (MTT; Sigma) to a purple formazan product. This reaction takes place when mitochondrial reductase enzymes are active. Cells were grown in 96-well plates (5×10^4 cells/well) for 24 h. Cultures were carried out at 37 °C in a humidified atmosphere with 5% CO_2 and incubated with the most active compounds in 100 μL of complete culture medium containing 25, 50, 75, 100, and 200 μM concentrations of each compound for 48 h. After incubation, the medium was removed and the cells were treated with 100 μL of 0.4 mg/mL MTT for 4 h at 37 °C. Subsequently, 100 μL of DMSO was added to the mixture. The solubilized formazan product was quantified with the help of a microtiter plate reader TECAN-Sunrise at 570 nm. In all cases, the compounds were dissolved in DMSO at the final concentration in the culture medium lower than 1%, a concentration that neither had a cytotoxic effect nor caused any interference with the colorimetric detection method. All experiments were performed at least three times. Untreated control parasites were used to calculate the relative proliferation. Dose−response curves were recorded and the CC_{50} values were determined using GraphPad Prism version 6.00 for Windows (GraphPad Software, La Jolla California, USA).[67] The results are presented as average SDs with SD below 10%.[30−33]

***In Vitro* Toxicity on Human Red Blood Cells (RBCs).** To evaluate the in vitro toxicological effect of the active 1,4-disubstitutedftalazines **2a**−**2h**, we used a model based on the lysis of red blood cells (RBCs), measuring the hemoglobin released in the supernatant fraction.[68] The hemoglobin released was measured using a spectrophotometer at 550 nm. Lysis of RBCs in 50% Alsever's solution were centrifuged at 800g for 10 min and then washed three times with saline solution to obtain RBCs. The synthesized compounds at three concentrations (0.1, 1, and 10 mM) were incubated with a 2% final suspension of RBCs at 37 °C for 45 min. The release of hemoglobin by an equal number of RBCs by hypotonic lysis in 0.05 vol of water was used as a 100% positive control, while RBCs treated with saline solution served as negative controls. Results were expressed as a hemolysis percentage (%) for each concentration of each tested compound.

Statistical Analysis. All experiments were performed at least three times. The results are expressed as mean ± SD. The ANOVA test was performed. Only post hoc Dunnett test $p < 0.01$ was considered to be statistically significant. The dose−response curves as well as the 50% growth inhibitory concentrations (IC_{50} or CC_{50}) of the compounds were determined by a nonlinear regression of individual experiments

calculated through computation with the GraphPad Prism v.5.02 software[67] program (Intuitive Software for Science, San Diego, CA, USA). The OriginPro2021b software package was employed for construction of graphic plots.[69]

Animal Ethics. All experiments adhered to the French guidelines for animal research and were approved by the ethical committee of the Instituto de Higiene (Universidad Central de Venezuela, Caracas).

Theoretical Calculations. All DFT calculations were carried out at the Copernico Cluster of the computational center at Science Faculty (Universidad Central Venezuela, Caracas, Venezuela). All theoretical calculations, in the gas phase, were performed by using density functional theory (DFT) with the Gaussian 09 quantum chemistry software.[65] To achieve a balance between the computational cost and the accuracy of the calculations, the B3LYP functional developed by Becke[63] in conjunction with the 6-31G(d,p) basis set[64] was used in the present study. By comparison purpose, the calculations were focused in the most active molecules including the 1,4-disubstituted phthalazines (**2a**, **2b**, **2d**, **2e**, **2f**, and **2h**), 1-substituted phthalazine-hydrazone (**1d**), 6-(N'-methylpiperazine)-3-(4-fluorophenyl)-1,2,4-triazolophthalazine (**3c**), N^1-aryl-2-trifluoromethyl-benzo[b]naphthyridin-4(1H)-ones (**5a**), and other non-active molecules such as 1-substituted phthalazine-hydrazone (**1p**), the 1,4-disubstituted phthalazine (**2c**), 6-chloro-3-phenyl-1,2,4-triazolophthalazine (**3a**), the 6-(N'-methylpiperazine)-3-(4-nitrofluorophenyl)-1,2,4-triazolophthalazine (**3c**), and the 2-(4-fluorophenyl)-quinazolin-4(3H)-one (**4b**). The geometry of the ground state of all mentioned ligands was optimized. The complexation ability of their optimized geometries with one molecule of iron(II) or iron(III) was determined through an interactive model. To obtain the corrected interaction energy, the basis set superposition error (BSSE) approach was incorporated into the calculations via the counterpoise (CP) method.[66] For the ligand−iron(II) and ligand−iron(II) complexes, the complexation energy was included in the calculation process. Theoretical complexation energies can be found in Table 5. The calculation output can be found in the Supporting Information.

Experimental Complexation Determination in Solution. The complexation ability of a selected group of active ligands (**1d**, **2a**, **2b**, **2c**, **2d**, **2e**, **2f**, **2h**, **3c**, **3d**, **4b**, and **5k**) with iron(III) was determined through a reported protocol with a few modifications by using UV−Vis spectroscopic measurements.[70−72] Titration with the iron(III) metal from 0 to 640 μM (10 concentrations) was performed at a constant ligand concentration: **1d** (200 μM), **2a** (140 μM), **2b** (120 μM), **2c** (200 μM), **2d** (100 μM), **2e** (200 μM), **2f** (150 μM), **2g** (100 μM), **2h** (82 μM), **3b** (100 μM), and **5k** (50 μM). Maximum absorption for each ligand can be found in Table S6. The association constant (K_a) was obtained from eq 1 that is derived from the equilibrium between iodine and dye in eq 2 as follows:

$$K_a = \frac{[Fe - ligand]}{[Fe^{3+}]^n \cdot [ligand]} \tag{1}$$

$$\mathbf{ligand} + n Fe^{3+} \rightleftharpoons ligand - (-Fe^{3+})_n \quad K_a \tag{2}$$
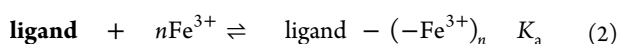
Complexation stoichiometry was determined for each ligand according to a reported procedure.[71] Results can be found in Figures S4−S7. A stoichiometry value of $n = 1$ was found for

the ligands **1d**, **3b**, **3k**, and CQ. The disubstituted phthalazin-hydrazones **2a**, **2b**, **2c**, **2d**, **2e**, **2f**, **2g**, and **2h** displayed a stoichiometry value of $n = 2$. Taking advantage of the discrete absorption of iron solution, association constants were determined from the $(A_{obs} - A_{ligand})/(A_{ligand})$ variation as a function of iron concentration according to eq 1 and the stoichiometry of the complexation. CQ was used as a positive control, whereas the 2-arylquinazolin-4(3H)-one **4b** was employed as a negative control. Some details can be found in the Supporting Information.

■ ASSOCIATED CONTENT

Ⓢ Supporting Information

The Supporting Information is available free of charge at https://pubs.acs.org/doi/10.1021/acsomega.1c05393.

> Full experimental details, further theoretical information, structure of 2-arylquinazolin-4(3H)-ones **4a−4t**, *in silico* data details for active compounds, full hemolysis data, absorption spectra in the absence and presence of iron(III), and output for the optimized structures of ligands and those derived from corresponding complexes with iron(II) and iron(III) (PDF)

■ AUTHOR INFORMATION

Corresponding Author

Angel H. Romero − *Caítedra de Química General, Facultad de Farmacia, Universidad Central de Venezuela, Caracas 1041-A, Venezuela*; Present Address: Present address: Grupo de Química Orgaínica Medicinal, Instituto de Química Biológica, Facultad de Ciencias, Universidad de la República, Iguaí 4225, 11400 Montevideo, Uruguay (A.H.R.); ◉ orcid.org/0000-0001-8747-5153; Email: angel.ucv.usb@gmail.com, angel.romero12@ucv.ve

Authors

María E. Acosta − *Unidad de Bioquímica, Facultad de Farmacia, Universidad Central de Venezuela, Caracas 1041-A, Venezuela*

Lourdes Gotopo − *Laboratorio de Síntesis Orgaínica, Escuela de Química, Facultad de Ciencias, Universidad Central de Venezuela, Caracas 1041-A, Venezuela*

Neira Gamboa − *Unidad de Bioquímica, Facultad de Farmacia, Universidad Central de Venezuela, Caracas 1041-A, Venezuela*

Juan R. Rodrigues − *Unidad de Bioquímica, Facultad de Farmacia, Universidad Central de Venezuela, Caracas 1041-A, Venezuela*

Genesis C. Henriques − *Unidad de Bioquímica, Facultad de Farmacia, Universidad Central de Venezuela, Caracas 1041-A, Venezuela*

Gustavo Cabrera − *Laboratorio de Síntesis Orgaínica, Escuela de Química, Facultad de Ciencias, Universidad Central de Venezuela, Caracas 1041-A, Venezuela*

Complete contact information is available at:
https://pubs.acs.org/10.1021/acsomega.1c05393

Author Contributions

theoretical calculations, G.J.C. provided the financial resource for theoretical calculations, and A.H.R. organized the investigation, analyzed all experimental and theoretical data, and prepared and revised the manuscript.

Notes

The authors declare no competing financial interest.

■ REFERENCES

(1) WHO. *World Malaria Report 2021* (https://www.who.int/publications/i/item/9789240040496) (accessed 20.01.2022).

(2) Paula, A. S.; Egan, E. S.; Duraisingh, M. T. Host-parasite interactions that guide red blood cell invasion by malaria parasites. *Curr. Opin. Hematol.* **2015**, *22*, 220−226.

(3) Francis, S. E.; Sullivan, D. J., Jr.; Goldberg, D. E. Hemoglobin Metabolism in the malarie parasite Plasmodium falciparum. *Ann. Rev. Microbiol.* **1997**, *51*, 97−123.

(4) Egan, T. J. Recent advances in understanding the mechanism of hemozoin (malaria pigment) formation. *J. Inorg. Biochem.* **2008**, *102*, 1288−1299.

(5) Hawley, S. R.; Bray, P. G.; Mungthin, M.; Atkinson, J. D.; O'Neill, P. M.; Ward, S. A. Relationship between antimalarial drug activity, accumulation, and inhibition of heme polymerization in Plasmodium falciparum in vitro. *Antimicrob. Agents Chemother.* **1988**, *42*, 682−686.

(6) Foley, M.; Tilley, L. Quinoline antimalarials: mechanisms of action and resistance. *Int. J. Parasitol.* **1997**, *27*, 231−240.

(7) Egan, T. J. Haemozoin Formation as a Target for the Rational Design of New Antimalarials. *Drug Des. Rev.* **2004**, *1*, 93−110.

(8) Fong, K. Y.; Wright, D. W. Hemozoin and antimalarial drug discovery. *Future Med. Chem.* **2013**, *5*, 1437−1450.

(9) Gorka, A. P.; de Dios, A.; Roepe, P. D. Quinoline drug-heme interactions and implications for antimalarial cytostatic versus cytocidal activities. *J. Med. Chem.* **2013**, *56*, 5231−5246.

(10) O'Neill, P. M.; Barton, V. E.; Ward, S. A.; Chadwick, J. *4-Aminoquinolines: Chloroquine, Amodiaquine and Next-Generation Analogues. Treatment and Prevention of Malaria. Milestones in Drug Therapy.* In: Staines, H.; Krishna, S. (eds) Springer: Basel, 2011.

(11) Valverde, E. A.; Romero, A. H.; Acosta, M. E.; Gamboa, N.; Henriques, G.; Rodrigues, J. R.; Ciangherotti, C.; López, S. E. Synthesis, β-hematin inhibition studies and antimalarial evaluation of new dehydroxy isoquine derivatives against Plasmodium berghei: A promising antimalarial agent. *Eur. J. Med. Chem.* **2017**, *148*, 498−520.

(12) Romero, A. H.; Acosta, M. E.; Gamboa, N.; Charris, J.; Salazar, J.; Lopéz, S. E. Synthesis β-hematin inhibition Studies and antimalarial evaluation of dehydroxy Isotebuquine derivates against Plasmodium berghei. *Bioorg. Med. Chem.* **2015**, *23*, 4755−4762.

(13) Foley, M.; Tilley, L. Quinoline antimalarials: mechanisms of action and resistance and prospects for new agents. *Pharmacol. Ther.* **1998**, *79*, 55−87.

(14) Lawrenson, A. S.; Cooper, D. L.; O'Neill, P. M.; Berry, N. G. Study of the antimalarial activity of 4-aminoquinoline compounds against chloroquine-sensitive and chloroquine-resistant parasite strain. *J. Mol. Model.* **2018**, *24*, 237.

(15) Callaghan, P. S.; Roepe, P. D. *The Biochemistry of Quinoline Antimalarial Drug Resistance. Handbook of Antimicrobial Resistance.* In: Gotte, M.; Berghuis, A.; Matlashewski, G.; Wainberg, M.; Sheppard, D. (eds), Springer: New York, NY, 2017.

(16) Peyton, D. H. Reversed chloroquine molecules as a strategy to overcome resistance in malaria. *Curr. Top. Med. Chem.* **2012**, *12*, 400−407.

(17) Kumar, S.; Guha, M.; Choubey, V.; Maity, P.; Bandyopadhyay, U. Antimalarial drugs inhibiting hemozoin (β-hematin) formation: A mechanistic update. *Life Sci.* **2007**, *80*, 813−828.

(18) Kumar, S.; Das, K.; Dey, S.; Maity, P.; Guha, M.; Choubey, V.; Panda, G.; Bandyopadhyay, U. Antiplasmodial activity of [(aryl)-arylsulfanylmethyl]Pyridine. *Antimicrob. Agents Chemother.* **2008**, *52*, 705−715.

(19) Fong, K. Y.; Sandlin, R. D.; Wright, D. W. Identification of β-hematin inhibitors in the MMV Malaria Box. *Int. J. Parasitol.* **2015**, *5*, 84−91.

(20) Ignatushchenko, V.; Winter, R. W.; Bachingerd, H. P.; Hinrischs, D. J.; Riscoe, M. K. Xanthones as antimalarial agents; studies of a possible mode of action. *FEBS Lett.* **1997**, *409*, 67−73.

(21) Vandekerckhove, S.; D'hooghe, M. Quinoline-based antimalarial hybrid compounds. *Bioorg. Med. Chem.* **2014**, *23*, 5098−5119.

(22) Hu, Y. Q.; Gao, C.; Zhang, S.; Xu, L.; Xu, Z.; Feng, L. S.; Wu, X.; Zhao, F. Quinoline hybrids and their antiplasmodial and antimalarial activities. *Eur. J. Med. Chem.* **2017**, *139*, 22−47.

(23) Sarkar, S.; Siddiqui, A. A.; Saha, S. J.; De, R.; Mazumder, S.; Banerjee, C.; Iqbal, M. S.; Nag, S.; Adhikari, S.; Bandyopadhyay, U. Antimalarial Activity of Small-Molecule Benzothiazole Hydrazones. *Antimicrob. Agents Chemother.* **2016**, *60*, 4217−4228.

(24) Verma, G.; Marella, A.; Shaquiquzzaman, M.; Akhtar, M.; Ali, M. R.; Alam, M. M. A review exploring biological activities of hydrazones. *J. Pharm. Bioallied Sci.* **2014**, *6*, 69−80.

(25) Romero, A. H. Role of Trifluoromethyl Substitution in Design of Antimalarial Quinolones: a Comprehensive Review. *Top. Curr. Chem.* **2019**, *377*, 9.

(26) Lawson, M. K.; Valko, M.; Cronin, M. T. D.; Jomovaí, K. Chelators in Iron and Copper Toxicity. *Curr. Pharmacol. Rep.* **2016**, *2*, 271−280.

(27) Romero, A. H.; Medina, R.; Alcala, A. M.; García-Marchan, Y.; Nuñez-Duran, J.; Leañez, J.; Mihoba, A.; Ciangherotti, C.; Serrano-Martín, X.; Lopez, S. E. Design, Synthesis, Structure-Activity relationship and Mechanism Studies of a Series of 4-chloro-1-phthalazinyl hydrazonas as potent agent against Leishmania braziliensis. *Eur. J. Med. Chem.* **2017**, *127*, 606−620.

(28) Romero, A. H.; Rodríguez, J.; García-Marchan, Y.; Leañez, J.; Serrano-Martín, X.; López, S. E. Aryl- or heteroaryl-based hydrazinylphthalazine derivatives as new potential antitrypanosomal agents. *Bioorg. Chem.* **2017**, *72*, 51−56.

(29) Romero, A. H.; López, S. E. In *silico* molecular docking of new potential 4-phthalazinyl-hydrazones on selected *T.cruzi* and *Leishmania* enzyme targets. *J. Mol. Graphics Modell.* **2017**, *76*, 313−329.

(30) Romero, A. H.; Rodríguez, N.; Oviedo, H.; Lopez, S. E. Antileismanial activity, mechanism of action study and molecular docking of 1,4-bis(substituted benzalhydrazino)phthalazines. *Arch. Pharm.* **2019**, *352*, 1800299.

(31) Romero, A. H.; Rodríguez, N.; Ramírez, O. G. Optimization of phthalazin-based aryl/heteroarylhydrazones to design new promising antileishmanicidal agents: Synthesis and biological evaluation of 3-aryl-6-piperazin-1,2,4-triazolo[3,4-a]phthalazines. *New J. Chem.* **2020**, *44*, 13807−13814.

(32) Romero, A. H.; López, S. E.; Rodríguez, N.; Oviedo, H. Antileishmanial activity, structure-activity relationship of series of 2-(trifluoromethyl)benzo[*b*][1,8]naphthyridin-4(1*H*)-ones. *Arch. Pharm.* **2018**, *351*, No. e1800094.

(33) Romero, A. H.; Rodríguez, N.; Oviedo, H. 2-Aryl-quinazolin-4(3H)-ones as an inhibitor of leishmania folate pathway: In vitro biological evaluation, mechanism studies and molecular docking. *Bioorg. Chem.* **2018**, *83*, 145−153.

(34) Zuzarte-Luis, V.; Mota, M. M. Parasite sensing of host nutrients and environmental cues. *Cell Host Microbe* **2018**, *23*, 749−758.

(35) Zucca, M.; Scutera, S.; Savoia, D. New chemotherapeutic strategies against malaria, leishmaniasis and trypanosomiases. *Curr. Med. Chem.* **2013**, *20*, 502−526.

(36) Romero, A. H.; Rodríguez, N.; López, S. E.; Oviedo, H. Identification of dehydroxy isoquine and isotebuquine as promising antileishmanial agents. *Arch. Pharm.* **2019**, *352*, 1800281.

(37) Kielmann, M.; Prior, C.; Senge, M. O. Porphyrins in troubled times: a spotlight on porphyrins and their metal complexes for explosives testing and CBRN defense. *New J. Chem.* **2018**, *42*, 7529−7550.

(38) Pearson, R. G. Hard and soft acids and bases, HSAB, part II: Underlying theories. *J. Chem. Educ.* **1968**, *45*, 643−648.

(39) Attanasio, D.; Dessy, G.; Fares, V. Synthesis and properties of Mo(VI), Mo(V), Mo(IV) and mixed valence Mo(V)Mo(IV) complexes with a binucleating Schiff's base. X-ray structure of the mononuclear cis-dioxo-aquo[1,4-dihydrazinophthalazine-bis-(salicylideneiminato)] molybdenum(VI) acetone solvate. *Inorg. Chim. Acta* **1985**, *104*, 99−107.

(40) Srivastava, S.; Pandey, O. P.; Sengupta, S. K. Binuclear oxovanadium(IV) complexes of phthalazine hydrazone ligands. *Transition Met. Chem.* **1996**, *21*, 262−265.

(41) Kogana, V. A.; Levchenkovb, S. I.; Popova, L. D.; Shcherbakov, I. A. 1-Hydrazinophthalazine based hydrazones and their transition metal complexes: Structure and biological activity. *Russ. J. Gen. Chem.* **2009**, *79*, 2767−2775.

(42) Mochon, M. C.; Gallego, M. C.; Perez, A. G. Salicylaldehyde-1-phthalazinohydrazone as an analytical reagent. *Talanta* **1986**, *33*, 627−630.

(43) Zhao, Y.; Lin, Z.; He, C.; Wu, H.; Duan, C. A "Turn-On" Fluorescent Sensor for Selective Hg(II) Detection in Aqueous Media Based on Metal-Induced Dye Formation. *Inorg. Chem.* **2006**, *45*, 10013−10015.

(44) Robichaud, P.; Thompson, L. K. Binuclear copper(II) complexes of some potentially sexadentate phthalazine hydrazone ligands. *Inorg. Chim. Acta* **1984**, *85*, 137−142.

(45) Wen, T.; Thompson, L. K.; Lee, F. L.; Gabe, E. J. Binuclear nickel(II) and cobalt(II) complexes of sexadentrate (N6) phthalazine ligands. Crystal and molecular structures of [.mu.-1,4-bis((6-methylpyridine-2-carboxaldimino)amino)phthalazine-4,N3,.mu.-N1,.mu.-N1A,N3A,N4A](.mu.-chloro)tetraaquodicobalt(II) trichloride-4.3-water, Co2C22H28Cl4N8O4.4.3H2O, and [.mu.-1,4-bis((6-methylpyridine-2-carboxaldimino)amino)phthalazine-N4,N3,.mu.-N1,.mu.-N1A,N3A,N4A](.mu.-chloro)tetraaquodinickel(II) trichloride-4.6-water, Ni2C22H28Cl4N8O4.4.6H2O. *Inorg. Chem.* **1988**, *27*, 4190−4196.

(46) Bullock, G.; Hartstock, F. W.; Thompson, L. K. Mononuclear and binuclear copper (II) complexes of some polyfunctional pyridyl phthalazines. *Can. J. Chem.* **1983**, *61*, 57−62.

(47) Ghedini, M.; De Munno, G.; Denti, G.; Manotti, A. M.; Tiripicchio, A. Synthesis and characterization of dinuclear copper(II) complexes. Crystal structure of aquatrichlorohydroxo-3,6-bis(2′-pyridyl)pyridazinedicopper(II). *Inorg. Chim. Acta* **1982**, *57*, 87−93.

(48) Dewan, C.; Thompson, L. K. Copper tetrafluoroborate complexes of the potentially binucleating ligand 1, 4-di (2′-pyridyl) aminophthalazine. Mononuclear and polynuclear derivatives. *Can. J. Chem.* **1982**, *60*, 121−132.

(49) Chung, L. Y.; Constable, E. C.; Dale, A. R.; Khan, M. S.; Liptrot, M. C.; Lewis, J.; Raithby, P. R. The transient template effect: chromium(III)-directed syntheses of metal-free macrocyclic ligands and crystal structure of 1,11-bis(2′-hydroxyethyl)-4,8;12,16;17,21-trinitrilo-1,2,10,11-tetra-azacyclohenicosa-2,4,6,9,12,14,18,20-octaene hydrochloride tetrahydrate. *J. Chem. Soc., Dalton Trans.* **1990**, 1397−1404.

(50) Budagumpi, S.; Kulkarni, N. V.; Sathisha, M. P.; Netalkar, S. P.; Revankar, V. K.; Suresh, D. K. Exploration on structure and anticonvulsant activity of transition metal complexes derived from an "end-off" compartmental bis-quinoxaline derivative with phthalazinyl-diazine as endogenous bridge. *Monatsh. Chem.* **2011**, *142*, 487−494.

(51) Barrios, A. M.; Lippard, S. J. Phthalazine-Based Dinucleating Ligands Afford Dinuclear Centers Often Encountered in Metalloenzyme Active Sites. *Inorg. Chem.* **2001**, *40*, 1060−1064.

(52) Rodríguez-Ciria, M.; Sanz, A. M.; Yunta, M. J. R.; Gómez-Contreras, F.; Navarro, P.; Saínchez-Moreno, M.; Boutaleb-Charki, S.; Osuna, A.; Castiñeiras, A.; Pardo, M.; Canoa, C.; Campayo, L. 1,4-Bis(alkylamino)benzo[g]phthalazines able to form dinuclear complexes of Cu(II) which as free ligands behave as SOD inhibitors and show efficient in vitro activity against Trypanosoma cruzi. *Bioorg. Med. Chem.* **2007**, *15*, 2081−2091.

(53) Romero, A. H.; Sojo, F.; Arvelo, F.; Calderón, C.; Morales, A.; López, S. E. Anticancer potential of new 3-nitroaryl-6-(N-methyl)-piperazin-1,2,4-triazolo[3,4-a]phthalazines targeting voltage-gated K+ channel: Copper-catalyzed one pot synthesis of 4-chloro-1-phthalazinyl-arylhydrazones. *Bioorg. Chem.* **2020**, *101*, 104031.

(54) Romero, A. H.; Romero, I. E.; Piro, O. E.; Echeverría, G. A.; Gotopo, L. A.; Moller, M. N.; Rodríguez, G. A.; Cabrera, G. J.; Castro, E. R.; López, S. E.; Cerecetto, H. E. A Photo-induced Partially Aromatized Intramolecular Charge-Transfer. *J. Phys. Chem. B* **2021**, *125*, 9268−9285.

(55) Baelmans, R.; Deharo, E.; Muñoz, V.; Sauvain, M.; Ginsburg, H. Experimental conditions for testing the inhibitory activity of chloroquine on the formation of beta-hematin. *Exp. Parasitol.* **2000**, *96*, 243−248.

(56) Sandlin, R. D.; Carter, M. D.; Lee, P. J.; Auschwitz, J. M.; Leed, S. E.; Johnson, J. D.; Wright, D. W. Use of the NP-40 detergent-mediated assay in discovery of inhibitors of beta-hematin crystallization. *Antimicrob. Agents Chemother.* **2011**, *55*, 3363−3369.

(57) Ncokazi, K. K.; Egan, T. J. A colorimetric high-throughput β-hematin inhibition screening assay for use in the search for antimalarial compounds. *Anal. Biochem.* **2005**, *338*, 306−319.

(58) Romero, A. H.; Salazar, J.; López, S. E. A Simple One-Pot Synthesis of 2-substituted 4(3H)-Quinazolinones from 2-Nitro-benzamides by using Sodium Dithionite. *Synthesis* **2013**, *45*, 2043−2050.

(59) Romero, A. H.; Salazar, J.; López, S. E. Synthesis of 2-(trifluoromethyl)benzo[b][1,8]naphthyridin-4(1H)-one derivatives using trifluoroacetimidoyl chlorides. *J. Fluorine Chem.* **2015**, *169*, 32−37.

(60) Peters, W. *Newapy and Drug Resistance in Malaria*; Academic Press: New York, 1970.

(61) http://www.swissadme.ch/index.php

(62) Daina, A.; Michielin, O.; Zoete, V. SwissADME: a free web tool to evaluate pharmacokinetics, drug-likeness and medicinal chemistry friendliness of small molecules. *Sci. Rep.* **2017**, *7*, 42717.

(63) Becke, A. D. A New Mixing of Hartree-Fock and Local Density-Functional Theories. *J. Chem. Phys.* **1993**, *98*, 1372−1377.

(64) Petersson, G. A.; Al-Laham, M. A. A Complete Basis Set Model Chemistry. II. Open-Shell Systems and the Total Energies of the First-Row Atoms. *J. Chem. Phys.* **1991**, *94*, 6081−6090.

(65) Frisch, M. J.; Trucks, G. W.; Schlegel, H. B.; Scuseria, G. E.; Robb, M. A.; Cheeseman, J. R.; Scalmani, G.; Barone, V.; Mennucci, B.; Petersson, G. A. et al. *Gaussian 09*; Revision A.1, Gaussian, Inc.: Wallingford, CT, 2009.

(66) Boys, S. F.; Bernardi, F. The calculation of small molecular interactions by the differences of separate total energies. Some procedures with reduced errors. *Mol. Phys.* **1970**, *19*, 553−566.

(67) Graph Pad Prism Software Inc. 4.02 for windows. May 17th 1992−2004.

(68) Mehta, R.; López-Berestein, G.; Hopfer, R.; Mills, K.; Juliano, R. L. Liposomal amphotericin B is toxic to fungal cells but not to mammalian cells. *Biochim. Biophys. Acta* **1984**, *770*, 230−234.

(69) *Origin(Pro)*, Version *8.0*. OriginLab Corporation: North-ampton, MA, USA.

(70) Bourson, J.; Pouget, J.; Valeur, B. Ion-Responsive Fluorescent Compounds. 4. Effect of Cation Binding on the Photophysical Properties of a Coumarin Linked to Monoaza- and Diaza-Crown Ether. *J. Phys. Chem.* **1993**, *97*, 4552−4557.

(71) Cai, J.; Hay, B. P.; Young, N. J.; Yang, X.; Sessier, J. L. A pyrrole-based triazolium-phane with NH and cationic CH donor groups as a receptor for tetrahedral oxyanions that functions in polar media. *Chem. Sci.* **2013**, *4*, 1560−1567.

(72) Hirose, K. Determination of Binding Constants, Chapter 2. *Analytical Methods in Supramolecular Chemistry*; John Wiley & Sons, 2006.